DROPLET FORMATION INSIDE A VENTURI LIQUID MIXER

S.L. Carnie[1] and M.R. Davidson[2]

The formation of a coarse photographic emulsion by entraining a hot oil phase into a cooler aqueous phase by a Venturi device is considered. The main focus is on understanding the mechanism and site of droplet formation in the device, as well as the time-scale of heat flow, to see if it is feasible to feed this emulsion directly to a homogenizer in a continuous process.

1.   Introduction

During the manufacture of colour photographic paper, the paper surface is overlaid with expensive dye-forming chemicals. These chemicals are dissolved in oil and are applied to the paper surface as an emulsion of small droplets in an aqueous phase. Previous MISG projects posed by Kodak have considered two stages of this process — the dissolution of the dyes in the oil phase (1995) and the homogenisation of the emulsion in an orifice disperser (1996).

In the first process, the oil must be heated to dissolve the dyes and currently these are mixed in a tank and stirred. The project goal was to determine the effectiveness of heating of a slurry passing through a microwave cavity. This proved quite challenging, mainly due to the large changes in slurry viscosity as the dye particles dissolved. The second project had to consider several mechanisms leading to the formation of very fine droplets, such as cavitation, shear and turbulent boundary layers.

This project concerns the intermediate process: the oil phase formed by the process studied in 1995 is combined with an aqueous phase in a Venturi device to form a coarse emulsion (the "pre-mix") before being stored in a tank and then pumped to the homogeniser studied in 1996.

Together these three projects constitute an effort to understand the whole mechanical process used to form photographic dispersions. The hope is that increased understanding will lead to improved outcomes such as smaller droplet

[1]Department of Mathematics, University of Melbourne, Parkville VIC, Australia 3052. Email carniesl@maths.mu.oz.au.

[2]Department of Chemical Engineering, University of Melbourne, Parkville VIC, Australia 3052. Email malcolmd@ariel.ucs.unimelb.edu.au.

size (mainly determined by the homogeniser step) or re-organizing the three steps as one continuous process, instead of the current series of batch processes.

Because the process involves droplet formation, there are some connections to the 1996 project but there are several differences.

1. The two phases start at different temperatures (the oil phase has to be heated to 140°C in order to dissolve the dyes; the aqueous phase is at 80°C).

2. The geometry is quite different since there is no orifice that the mixture is forced through.

3. The Venturi device involves much lower pressures so some of the extreme conditions present in the homogeniser are not encountered here.

A schematic diagram of the device is shown in Figure 1. The aqueous phase acts as the motive fluid in a pump and entrains the oil which sits in a small tank feeding into the mixing chamber. The rate of entry of the oil is controlled by a valve and is set to achieve the desired volume ratio required by the formulation. The mixture exits the Venturi device into a pipe which leads to a holding tank. Some final mixing by stirring is done in the tank but the focus of this project is on the Venturi device.
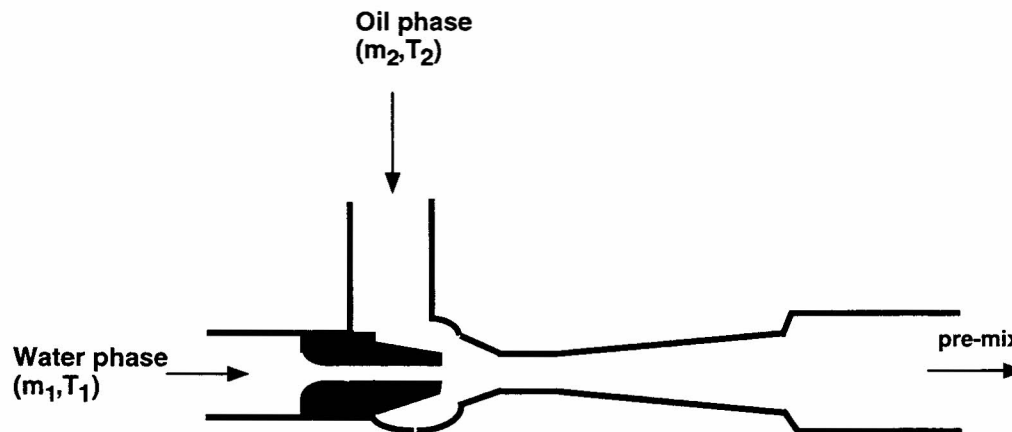

Figure 1: Schematic of a Venturi liquid mixer (not to scale). The two fluids enter the device with mass fluxes m_1, m_2 at temperatures T_1, T_2.

The device currently works satisfactorily and produces a distribution of drop sizes, ranging from 1–10 μm. Since it is only a pre-mix for another stage of the process, the exact distribution is perhaps not vital. Ideally, we would like to be able to predict a drop size distribution for the mixture leaving the device.

2. Material properties

Since the material produced in this process forms the input to the homogeniser, we have taken the same set of standard values for viscosity etc. as used in 1996. Note that these all are taken at 80°C. The temperature dependence of the oil viscosity and interfacial tension was not available so the team had to neglect such effects. One might expect the oil viscosity to be substantially lower at 140°C. Although the mixture is known to be only slightly shear thinning, it was not known directly whether each phase was Newtonian so this was assumed. It would be desirable for more information of this type to be determined if the problem is to be studied further.

thermal diffusivity (aqueous)	2×10^{-3} cm^{2}s^{-1}
thermal diffusivity (oil)	3×10^{-4} cm^{2}s^{-1}
specific heat (aqueous)	3.95×10^3 J kg^{-1} K^{-1}
specific heat (oil)	1.95×10^3 J kg^{-1} K^{-1}
viscosity (aqueous)	15 cP
viscosity (oil)	50 cP
viscosity (bulk)	40 cP
specific gravity (aqueous)	1.0
specific gravity (oil)	1.0
interfacial tension	10 dyne/cm

Table 1: Typical values used by the MISG of physical properties at 80°C.

3. Flow characteristics

The flow is determined by the geometry of the device, the imposed mass flow rates and the material properties listed above. The aqueous phase exits the nozzle of diameter 5 mm at a rate of 38 kg/min. The mass flow rate of the oil is adjusted to be 12 kg/min, to produce a mixture with volume ratio of roughly 3:1. The Venturi consists of a contraction section 16.5 mm long, a throat of diameter 10 mm and length 22.5 mm and a diffuser section of length 30 mm, leading to a pipe of diameter 25 mm.

Using these values we find a nozzle velocity of 32 ms^{-1} with a Reynolds number (based on the diameter) of 10^4. Using the combined mass flow rate, we get a velocity in the throat of 10 ms^{-1} with a Reynolds number of 2500 in the throat and about 1000 in the exit pipe.

From these considerations, we clearly have a turbulent jet emerging from the nozzle, turbulent flow in the throat and possibly transition back to laminar flow

in the pipe. We can also estimate residence times for the droplets: about 2 ms in the throat and about 4 ms in the diffuser section of the Venturi device, giving a total residence time of at least 6 ms.

4.   The temperature issue

The simplest issue to deal with is that involving the equilibration of temperature between the two liquids. In particular, has the temperature equilibrated by the time the mixture leaves the Venturi device or is the pipe flow required for equilbration?

Using the specific heats and densities from Table 1 and a mass ratio of 3:1, a simple heat balance gives a temperature for the mixture (taking the heat capacity for the mixture to be the weighted average of the components) of 88°C compared to the observed final temperature in the holding tank of 83°C. So the temperature assuming instant mixing is not far from the final temperature because the heat capacity of the oil is fairly low.

So the main issue is: do the drops have enough time to lose heat to the fluid while in the Venturi? We must consider both convective and conductive heat transfer from the drop to the fluid.

Convective heat transfer is a consequence of relative velocity differences between the drop and the surrounding fluid that can sweep heat away from the drop surface. Since the drops are small, they will closely follow the velocity of the fluid, and the particle Reynolds number based on relative velocity and drop diameter will be small. In that case, the equation of motion of a spherical drop involving only the dominant drag force is

$$\frac{\rho_D 4\pi R^3}{3}\frac{dU_D}{dt} = -6\pi\eta_C R(U_D - U_C) \tag{1}$$

where the right hand side of equation (1) is the Stokes drag on a drop with velocity U_D in a fluid of velocity U_C. The general equation of motion containing extra terms due to added mass and the Basset history term can be found in Clift *et al.* (1978). Equation (1) can be rewritten as

$$\frac{dU_D}{dt} = -\frac{U_D - U_C}{t_p} \tag{2}$$

where $t_p = \frac{2\rho_D R^2}{9\eta_C}$ is known as the particle relaxation time. When t_p is very small compared with a time scale of the flow (L/U) then $U_D \approx U_C$. This ratio of time scales is called the Stokes number, *St*. For a drop of diameter 1 micron

and using the residence time as the characteristic time, we find

$$St = \frac{2R^2 \rho_D / 9\eta_C}{L/U} \approx 10^{-5} \tag{3}$$

so that the drop is essentially carried at the local velocity very soon after formation. This suggests that convective heat transfer is not an important mechanism. According to Clift *et al.* (1978), the retention of the extra terms omitted in equation (1) can increase the time required for the particle to match the fluid velocity substantially. For example, to reach 90% of U_C can take times of roughly 100 t_p — still not enough to change the conclusion reached here.

Using the thermal diffusivities in Table 1 and a radius of 1 μm, one gets a diffusive timescale given by

$$t_{diff} = \frac{R^2}{\alpha} \tag{4}$$

to be around 0.01 ms. In light of the residence times of around 5 ms, there appears to be ample time for the drops to equilibrate with the aqueous phase. Even drops of 10 μm have (just) enough time to equilibrate. We conclude that temperature equilibration is not a relevant issue in a redesign of the process.

5.   Droplet formation by the mean flow

As mentioned above, the flow from the nozzle is best described as a turbulent jet. Strictly speaking, we have a confined jet because the throat of the Venturi device is so close to the nozzle. For an exact treatment such flows must be studied numerically so we shall be forced to treat the jet as free (unconfined) for the purposes of analytic investigations. For this case there are self-similar solutions for the laminar jet, which when rescaled with an eddy viscosity (Schlichting, 1968; Rajaratnam, 1976), give reasonable agreement with experiment for the mean velocity profile of a free axisymmetric jet (Townsend, 1976). For nice pictures of free axisymmetric jets at Reynolds numbers similar to those here, see Yule (1978) and Dahm and Dimotakis (1987). Thanks to the capabilities of the *Fastflo* package (Luo *et al.*, 1996), we are able to supplement estimates from a free jet model with numerical simulations of the confined jet using a simple turbulence model.

5.1   The mean flow

The self-similar solutions for the velocity field of an axisymmetric free jet assuming the existence of an eddy viscosity take the form (Schlichting, 1968; Rajaratnam, 1976)

$$U = \frac{3}{8\pi} \frac{K}{\nu_t x} \frac{1}{(1 + \xi^2/4)^2} \tag{5}$$

$$V = \frac{1}{4} \sqrt{\frac{3}{\pi}} \frac{\sqrt{K}}{x} \frac{\xi - \xi^3/4}{(1 + \xi^2/4)^2} \tag{6}$$

where

$$\xi = \frac{1}{4} \sqrt{\frac{3}{\pi}} \frac{\sqrt{K}}{\nu_t} \frac{r}{x} \equiv \Gamma \frac{r}{x} \tag{7}$$

is the scaled similarity variable,

$$K = 2\pi \int r U^2 dr \tag{8}$$

is the kinematic momentum flux and

$$\nu_t = 0.0161 \sqrt{K} \tag{9}$$

is an empirically determined relation for the eddy viscosity ν_t. Here U, V are the velocity components in the x (downstream) and r (transverse) directions. A sketch of the streamlines is given in Figure 2.

In light of equation (9), the useful parameter Γ defined above has the value 15.17. For the conditions described in Section 3, we have the constants

$$K = 2.01 \times 10^{-2} \text{ m}^4 \text{s}^{-2} \tag{10}$$

$$\nu_t = 2.268 \times 10^{-3} \text{ m}^2 \text{s}^{-1} \tag{11}$$

Note that the eddy viscosity is two orders of magnitude larger than the molecular viscosity in this flow.

From this solution, we first determine the position of maximum shear on each streamline. Under the conditions used to derive the similarity solution, the shear is dominated by $\frac{\partial U}{\partial r}$. By using the equation for the Stokes streamfunction

$$\Psi = \nu_t x \frac{\xi^2}{1 + \xi^2/4} \tag{12}$$

we can eliminate x in favor of Ψ and ξ in the expression for $\frac{\partial U}{\partial r}$. Hence we find the maximum shear along each streamline. This occurs at $\xi = 2$ which gives $V = 0$ i.e. where the streamline turns from entrainment to entering the jet. This represents a cone of maximum shear.

The value of the maximum shear rate along each streamline is given by

$$G_{max} = 2\frac{(\Gamma \nu_t)^3}{\Psi^2}. \tag{13}$$

The value of Ψ varies from lower values near the axis (corresponding to large shear rates) to large values away from the axis.
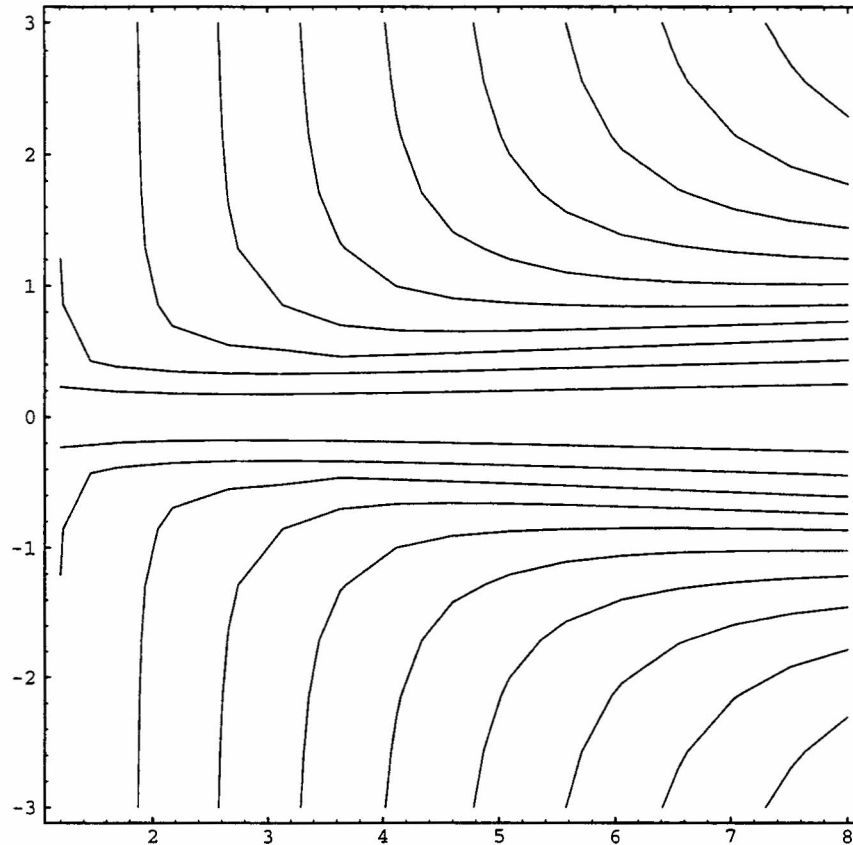
Figure 2: Streamlines of the axisymmetric jet.

5.2   The breakup criterion

Assuming that the droplets are being formed in the shear layer at the edge of the jet, we then see that as the oil phase is entrained it is subject to a range of shear rates depending on how close to the nozzle the blobs of oil approach as they enter the main stream. For each shear rate G_{max} we associate a drop size according to the criterion used in the 1996 report.

A drop of radius R will break when the capillary number

$$Ca = \frac{G\eta_C R}{\gamma} \tag{14}$$

exceeds a critical value Ca_{crit}. The capillary number represents the ratio of viscous stresses ($\eta_C G$) to the Laplace pressure difference (γ/R) which resists drop deformation.

The critical capillary number depends on the flow type (e.g. simple shear versus elongational flow) and on the viscosity ratio η_D/η_C of the dispersed (oil) to continuous (aqueous) phase. The flow at the edge of the jet is close to simple shear and, typically, $\eta_D/\eta_C \sim 3$. In that case, $Ca_{crit} \sim 0.1$–0.2 (Stone, 1994). Thus we expect that the rate of strain G must satisfy

$$G > G_{crit} \sim 10^5 \text{ s}^{-1} \tag{15}$$

for drops larger than $1\ \mu$m to break. As in 1996, we are forced to apply a criterion derived from the steady shear regimes studied in Stone (1994) to an unsteady turbulent flow. In slight defense of this, pictures of the jet in Yule (1978) show the first nozzle diameter downstream to be much more steady than the fully-developed turbulence further downstream.

Using a critical capillary number of 0.1 and using equation (13) in equation (14), we get (for the conditions considered here)

$$R = 802\Psi^2 \tag{16}$$

where both R and Ψ are in SI units.

To proceed we must consider the details of the geometry. It is usual (Schlichting, 1968) to place the origin of the streamfunction behind the start of the nozzle at some virtual origin. Hinze suggested this be located at a position $1.2\ r_0$ (i.e. 3 mm) behind the opening of the nozzle, in order to better fit his data at large distances downstream ($x/r_0 \geq 10$). We will follow this suggestion for the moment although it must be recognized that this is a rather dubious procedure in order to make what is really a far-field solution physical in the near-field (with no virtual origin we run the risk of infinite shear rates and drops of zero size).

We have used such a coordinate system in Figure 3 with the downstream coordinate (scaled by r_0) starting at the virtual origin and reaching 1.2 at the opening. The vertical coordinate gives r (scaled by r_0) with values of 1 at the inside corner of the nozzle. In these coordinates the outside corner of the nozzle is at $(1.2, 2)$, the start of the contraction section of the Venturi is at $(3.6, 3)$ and the start of the throat is at $(7.8, 2)$.

The oil must pass along the streamlines between that which grazes the outside corner of the nozzle and that which grazes the entry of the Venturi (not the throat). In this picture the smallest drops are produced by the streamlines passing closest to the nozzle and feeling the largest shear. The largest drops are those whose streamlines just enter the Venturi opening. Using these points to determine the values of the streamfunction, we find the smallest value of Ψ to be 2.5×10^{-5} SI units, leading to a drop size of $0.58\ \mu$m and the largest value of Ψ to be 8×10^{-5} SI units, leading to a drop size of $5.1\ \mu$m. Of course, given the
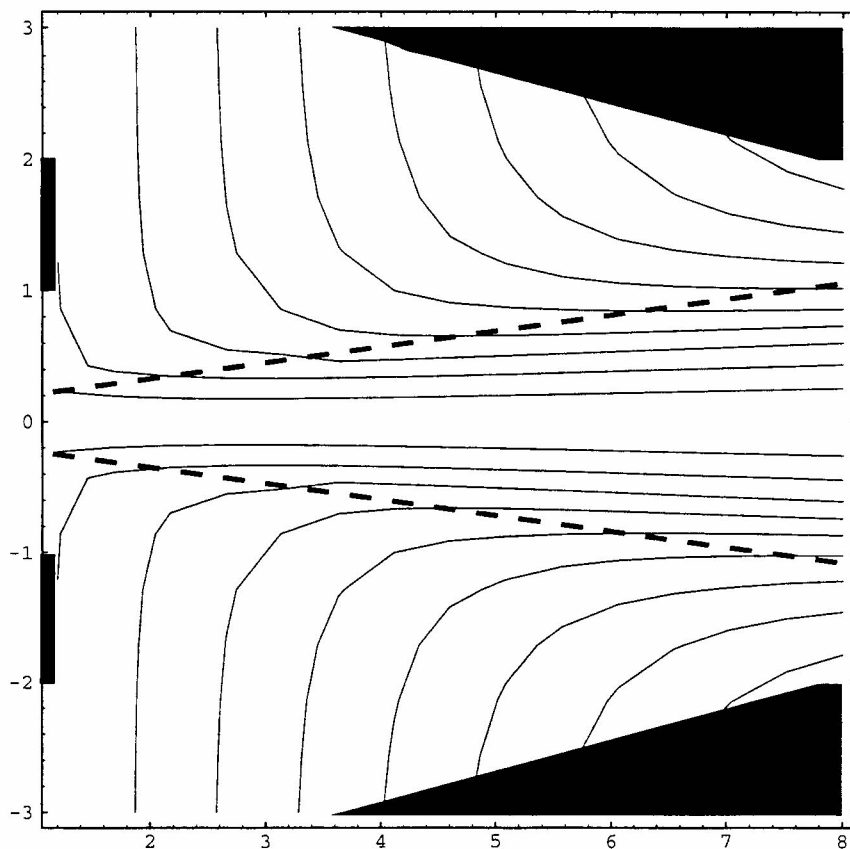
Figure 3: Streamlines in the region from the nozzle to the start of the throat of the Venturi . Coordinates refer to a virtual origin a distance 1.2 r_0 inside the nozzle and are scaled by r_0. The dashed lines show the cone of maximum shear.

many assumptions made in this analysis these numbers must be taken as rather approximate. For example, one could use for the upper cutoff the streamline that intersects the cone of maximum shear and the plane of the throat entrance — this gives a maximum drop size of 6.3 μm.

5.3   A droplet size distribution

Knowing the drop size produced along each streamline, we now calculate the volume flux of oil phase in each streamtube to produce a population distribution of drops, either in terms of the number of drops of each size or the volume fraction at each size.

From the properties of the Stokes streamfunction, the flux in the streamtube bounded by Ψ and $\Psi + d\Psi$ is just $2\pi d\Psi$. Given a fixed volume fraction λ of oil, the flux of oil is $2\lambda\pi d\Psi$. Since each value of Ψ corresponds in our treatment to a dropsize R, we get the volume distribution of drops

$$P_V(R)dR = 2\pi\lambda\frac{d\Psi}{dR}dR \qquad (17)$$

and the number distribution of drops

$$P_N(R) = P_V(R)/(4\pi R^3/3). \qquad (18)$$

Using equation (16), we find

$$P_N(R) \propto R^{-7/2}. \qquad (19)$$

The disc centrifuge particle sizer used by Kodak appears to measure the number distribution so in principle this is a testable prediction of the model. The experimental curves show a distribution of roughly lognormal shape with a sharp leading edge at small drop sizes and a gentle tail at larger drop sizes. Our rather rough model gives a monotonically decreasing distribution cutoff at small drop sizes due to the nozzle and at large sizes due to the Venturi with a somewhat faster decay than the measured distribution.

6. Droplet formation by turbulent fluctuations

The other chief mechanisms cited for droplet breakup in turbulent flow (Walstra, 1983) invoke concepts from the theory of isotropic turbulence due to Kolmogorov. Since all relations in this area have unknown constant factors, we shall be content with order of magnitude estimates.

In this picture, we have two mechanisms depending on the size of the drop compared to the so-called Kolmogorov length scale l_K. This length scale is determined from the kinematic viscosity of the fluid ν and the mean turbulent energy dissipation ϵ by

$$l_K = \nu^{3/4}\epsilon^{-1/4}. \qquad (20)$$

6.1 Inertial forces

For drops larger than this scale, inertial forces are the dominant mechanism for drop breakup with the turbulent pressure fluctuations competing with the Laplace pressure in the drop. In this picture, breakup occurs if

$$\Delta p \approx \rho\overline{U'^2} \approx \frac{2\gamma}{R} \qquad (21)$$

where $\overline{\frac{1}{2}U'^2}$ is the mean kinetic energy associated with velocity fluctuations in one direction. This is related to the overall turbulent kinetic energy k by

$$k = \frac{1}{2}(\overline{U'^2} + \overline{V'^2} + \overline{W'^2}) = \frac{3}{2}\overline{U'^2} \tag{22}$$

assuming isotropic turbulence. As discussed in Yule (1978) and Simpson (1975), this is unlikely to be valid both close to the nozzle where coherent structures are clearly evident and in the throat, where wall effects would be expected to disturb isotropy. However, the simplifying assumption of isotropy is frequently made in the absence of more precise knowledge.

Calculations were done with a renormalization group $k - \epsilon$ model of turbulence (Yakhot and Orszag, 1986) using the package *Fastflo* on the geometry shown in Figure 1 and a nozzle velocity of 30 ms^{-1}. An output of this model is the turbulent kinetic energy k as a scalar field. In the shear layer near the jet entry, values of 63 m^{2}s^{-2} were found. Substitution into equation 22 gives a drop size of about 0.5 μm.

In order to find the Kolmogorov scale, we used the numerical calculation with *Fastflo* to find a value for ϵ. It is largest in the shear layer at the edge of the jet and to a noticeable extent near the wall in the throat region. The largest value was 5×10^5 m^{2}s^{-3}, which can be compared with a value of 10^5 m^{2}s^{-3} given by Walstra (1983) for an Ultra Turrax mixer. Such a value gives a Kolmogorov scale equal to 9 μm. This means that the inertial mechanism is a consistent and plausible mechanism for droplet breakup for sizes greater than about 10 μm.

Monocolour contour plots of k and ϵ from the numerical computation are not as illuminating as the colour contour plots shown at the final day of the MISG workshop and so they are not given here.

6.2   Viscous forces

This leaves another mechanism to consider: the shear due to velocity fluctuation contained in eddies at the Kolmogorov scale. These eddies are responsible for most of the energy dissipation in the flow. When we equate this dissipation with dissipation by turbulent shear

$$\epsilon \approx \nu_C G^2 \tag{23}$$

we get turbulent shear rates of 2×10^5 s^{-1} which by our critical capillary number criterion can produce drops of radius 0.5–1 μm (depending on Ca_{crit}), yet again!

6.3 Timescales

Finally, we have to consider whether the turbulent eddies last long enough to break the droplets. The deformation time

$$t_{def} = \frac{\eta_D R}{\gamma} \tag{24}$$

is about 5 μs for a 1 μm drop. This should be compared with typical residence times given in Section 3 for the case of breakage by the mean flow and with eddy lifetimes for the case discussed here. With residence times in the entry section of order ms, there is enough time to break drops up to 100 μm in size before the throat — any larger drops that survive must get broken in the throat.

The lifetime of an eddy of the size of the Kolmogorov scale is given by

$$t_K \approx \nu_C^{1/2} \epsilon^{-1/2} \approx 6 \ \mu s \tag{25}$$

so the smallest turbulent eddies do have (just) enough time to break drops of 1 μm size.

7.   Some extensions

We mention two possible ways to extend the treatment given above, especially the methods of Section 5.

7.1   The annular shear layer

One objection to the use of the equations for the self-similar jet is that such self-similar structure only sets in after about 10 diameters downstream, which in our case is well past the throat. To get a feel for the near-field flow, one can look at more empirical expressions describing the flow closer to the nozzle.

According to Rajaratnam (1976), the mean axial flow near the nozzle can be described roughly as following. Inside a region $r \le r_{in}$ (the potential core), the axial velocity U is equal to the nozzle velocity U_0. Outside a region $r \ge r_{out}$, the velocity is zero (or the outer stream velocity in the case of a compound jet). In between we have an annular shear layer described by

$$\frac{U}{U_0} = \frac{1}{2}(1 - cos\pi\zeta) \tag{26}$$

where ζ is a scaled transverse coordinate

$$\zeta = \frac{r_{out} - r}{r_{out} - r_{in}}.$$ (27)

From this it is easy to find the cone of maximum shear at $\zeta = \frac{1}{2}$.

Empirically, the boundaries of the shear layer are found to be given by

$$\frac{r_{in}}{r_0} = 0.95 - 0.097 \frac{x}{r_0}$$ (28)

$$\frac{r_{out}}{r_0} = 1.07 + 0.158 \frac{x}{r_0}$$ (29)

i.e. the boundaries both have virtual origins behind the actual nozzle. Using these expressions and computing the maximum shear as before, we find a shear rate that can break a drop of radius 0.4 μm, which is comfortingly close to our previous estimates.

7.2   Swirling jets

Finally, we mention the possibility of studying jets with swirl. The addition of swirl (azimuthal velocity) to a jet makes it spread faster and enhances mixing (Simpson, 1975). We would not want the jet to spread so fast that it doesn't enter the throat so there is a limit to the amount of swirl that is beneficial. Equations for a swirling jet are available (Rajaratnam, 1976) for such an investigation, if desired.

8.   Conclusions

We have considered the mechanisms of droplet formation in a Venturi liquid mixer. We conclude that temperature equilibration is not a significant factor in any redesign of the current process. The overall picture that emerges is that the oil phase is entrained by a circular jet, droplets are formed both by shear in the mean flow and by turbulent fluctuations. The smallest drops are formed closest to the nozzle and the largest ones near the throat entry. The predicted dropsize distribution is qualitatively similar to the measured one. Any large drops entering the throat are broken by shear near the wall of the throat. Further study on the effect of swirl is warranted.

We close with a quote from Simpson (1975): "Trying to understand drop or bubble transport processes can be a frustrating experience".

9. Notation

Ca — Capillary number
G — shear rate
k — turbulent kinetic energy
K — kinematic momentum flux of jet
l_K — Kolmogorov length scale
r_0 — nozzle radius
P_N — number distribution of drops
P_V — volume distribution of drops
r — transverse coordinate
r_0 — nozzle radius
r_{in} — boundary of potential core
r_{out} — boundary of outer region of annular shear layer
R — droplet radius
St — Stokes number
t_{def} — deformation time of droplet
t_{diff} — diffusion time for heat
t_K — lifetime of eddy at Kolmogorov scale
t_p — particle relaxation time
U — axial velocity
U' — velocity fluctuation
U_C — velocity of continuous (aqueous) phase
U_D — velocity of droplet phase
U_0 — velocity of jet at nozzle
V — transverse velocity
x — axial coordinate
α — thermal diffusivity
γ — interfacial tension
Γ — parameter appearing in ξ
ϵ — turbulent energy dissipation
λ — volume fraction of oil in emulsion
ν_C — kinematic viscosity of continuous (aqueous) phase
ν_D — kinematic viscosity of droplet phase
ν_t — turbulent eddy viscosity
ρ_D — density of droplet phase
η_C — viscosity of continuous (aqueous) phase
η_D — viscosity of droplet phase
ξ — similarity variable
Ψ — Stokes streamfunction
ζ — scaled tranverse coordinate in annular shear layer

Acknowledgements

References

R. Clift, J.R. Grace and M.E. Weber, *Bubbles, Drops and Particles* (Academic Press, 1978).

W.J.A. Dahm and P.E. Dimotakis, "Measurements of entrainment and mixing in turbulent jets", *AIAA Journal* **25** (1987), 1216–1223.

X. Luo, Z. Zhu and N. Stokes, "Turbulence modelling in *Fastflo*", *Proc. Australian Engineering Mathematics Conf. – AEMC96*, Sydney 1996.

N. Rajaratnam, "Turbulent jets", volume **5** of *Developments in Water Science* (Elsevier, New York, 1976).

H. Schlichting, *Boundary Layer Theory*, 6th Ed., (McGraw-Hill, New York, 1968).

L.L. Simpson, "Industrial turbulence modelling", *Turbulence in Mixing Operations: Theory and Application to Mixing and Reaction* (Academic Press, 1975).

H.A. Stone, "Dynamics of drop deformation and breakup in viscous fluids", *Ann. Rev. Fluid Mech.* **26** (1994), 65–102.

A.A. Townsend, *The Structure of Turbulent Shear Flow*, 2nd Ed., (Cambridge University Press, 1976).

P. Walstra, "Formation of emulsions", *Encyclopedia of Emulsion Technology, Vol 1. Basic Theory* (M. Dekker, 1983), 57–127.

V. Yakhot and S.A. Orszag, "Renormalization group analysis of turbulence: 1. Basic theory", *J. Sci. Comput.* **1** (1986).

A.J. Yule, "Large scale structure in the mixing layer of a round jet", *J. Fluid Mech.* **89** (1978), 413–432.